Highly Efficient Ethylene/Norbornene Copolymerization by *o*-Di(phenyl)phosphanylphenolate-Based Half-Titanocene Complexes

Xiao-Yan Tang,[1,2] Yong-Xia Wang,[1] Bai-Xiang Li,[1] Jing-Yu Liu,[1] Yue-Sheng Li[1]

[1]State Key Laboratory of Polymer Physics and Chemistry, Changchun Institute of Applied Chemistry, Chinese Academy of Sciences, Changchun 130022, China
[2]Graduate School of the Chinese Academy of Sciences, Changchun Branch, China
Correspondence to: J.-Y. Liu (E-mail: ljy@ciac.jl.cn)

Received 25 September 2012; accepted 10 December 2012; published online 8 January 2013
DOI: 10.1002/pola.26528

ABSTRACT: A series of *o*-di(phenyl)phosphanylphenolate-based half-titanocene complexes $CpTiCl_2[O\text{-}2\text{-}R^1\text{-}4\text{-}R^2\text{-}6\text{-}(Ph_2P)C_6H_2]$ (Cp = C_5H_5, **2a**: $R^1 = R^2 = H$; **2b**: $R^1 = F$, $R^2 = H$; **2c**: $R^1 = Ph$, $R^2 = H$; **2d**: $R^1 = SiMe_3$, $R^2 = H$; **2e**: $R^1 = {}^tBu$, $R^2 = H$; **2f**: $R^1 = R^2 = {}^tBu$) have been synthesized in high yields (65–87%) by treating $CpTiCl_3$ with 1.0 equiv of the deprotonated ligands in THF. The ^1H and ^{31}P NMR spectra indicated that the phosphorus is not coordinated to titanium in complexes **2a–c**, but is coordinated to titanium in complexes **2d–f**. Structures for **2c–f** were further confirmed by X-ray crystallography. Complex **2c** is essentially a four-coordinate tetrahedral geometry, whereas complexes **2d-f** adopt five-coordinate distorted square–pyramid geometry around the titanium center. All complexes exhibited low to moderate activities toward homopolymerization of ethylene. Excitingly, they displayed excellent ability to copolymerize ethylene with norbornene, and catalytic activity was more than 100 times larger than that of ethylene homopolymerization in the case of $Ph_3CB(C_6F_5)_4/{}^iBu_3Al$ as cocatalyst, affording the copolymers with high comonomer incorporations. Moreover, DFT calculations study had been performed to shed light on the active species and the fundamental role of NBE in improving the catalytic activity. © 2013 Wiley Periodicals, Inc. J. Polym. Sci., Part A: Polym. Chem. **2013**, *51*, 1585–1594

KEYWORDS: calculations; catalysts; copolymerization

INTRODUCTION Design and synthesis of well-defined, single-site group IV metal catalysts for olefin polymerization has attracted considerable attention.[1] Among them, half-metallocene-type metal complexes are of particular interest and importance from the industrial point of view. Following the success of half-sandwich titanium amide (constrained geometry) catalysts (CGC), a great deal of examples of $Cp'M(L)X_2$ have been reported.[2–20] Most of them were supported by bi-, tri-, and tetradentate chelating and anionic ligands containing, in various combinations, nitrogen and oxygen hard donors. In contrast, anionic chelating ligands incorporating L-type soft donors such as phosphine donors have been much less explored.[18,19] Nevertheless, recent work on early transition-metals such as Group IV metal complexes strongly suggests that the use of ancillary ligands with softer L donors, such as phosphorus and sulfur, may offer beneficial stabilization of the highly reactive metal center.[21]

We have become interested in the synthesis of cationic group IV compounds supported by bidentate ligands with softer donor atoms to evaluate their potential application in polymerization catalysis.[22] As part of our investigation of *o*-di(phenyl)phosphanylphenolate ligands in homogeneous polymerization catalysis, we were interested in combining the high polymerization activity of *o*-di(phenyl)phosphanylphenolate ligands with cyclopentadienyl group to produce more active catalysts and more interesting polymerization behavior. Although [O, P]-type half-titanocene complexes were first published in 1996,[19] their potential application in polymerization catalysis remains virtually unexplored.

With this in mind, we initiated the studies of synthesizing and characterizing some titanium complexes for precise, controlled olefin (co)polymerization. Herein, we thus describe the synthesis and characterization of some novel *o*-di(phenyl)phosphanylphenolate-based half-titanocene complexes $CpTiCl_2[O\text{-}2\text{-}R^1\text{-}4\text{-}R^2\text{-}6\text{-}(Ph_2P)C_6H_2]$ (Cp = C_5H_5, **2a**: $R^1 = R^2 = H$; **2b**: $R^1 = F$, $R^2 = H$; **2c**: $R^1 = Ph$, $R^2 = H$; **2d**: $R^1 = SiMe_3$, $R^2 = H$; **2e**: $R^1 = {}^tBu$, $R^2 = H$; **2f**: $R^1 = R^2 = {}^tBu$), and explored their application in ethylene polymerization and ethylene/NBE copolymerization. These complexes displayed excellent ability to copolymerize ethylene with norbornene (NBE), and catalytic activity was more than one order of magnitude higher than that of ethylene homopolymerization, especially in the case of $Ph_3CB(C_6F_5)_4/{}^iBu_3Al$ as cocatalyst.

Additional Supporting Information may be found in the online version of this article.

EXPERIMENTAL

General Procedures and Materials

All manipulation of air- and/or moisture-sensitive compounds was carried out under a dry argon atmosphere by using standard Schlenk techniques or under a dry argon atmosphere in an MBraun glovebox unless otherwise noted. All solvents were purified from an MBraun SPS system. The ^{1}H NMR data of the ligands and complexes used were obtained on a Bruker 300-MHz spectrometer; the ^{31}P NMR and ^{13}C NMR data of the complexes were obtained on a Bruker 400− and 600-MHz spectrometer, respectively, at ambient temperature, with $CDCl_3$ as the solvent (dried by MS 4 Å). The NMR data of the polymers were obtained on a Varian Unity-400-MHz spectrometer at 135 °C, with *o*-$C_6D_4Cl_2$ as a solvent. Elemental analyses were recorded on an elemental Vario EL spectrometer. The weight-average molecular weights (M_w) and the polydispersity indices of polymer samples were determined at 150 °C by a PL-GPC 220 type high-temperature chromatograph equipped with three Plgel 10-μm Mixed-B LS-type columns. 1,2,4-Trichlorobenzene was used as the solvent at a flow rate of 1.0 mL/min. The calibration was made by polystyrene standard EasiCal PS-1 (PL). $CpTiCl_3$ were purchased from Aldrich. Modified methylaluminoxane (MMAO, 7% aluminum in heptane solution) was purchased from Akzo Nobel Chemical. Commercial ethylene was directly used for polymerization without further purification. The other reagents and solvents were commercially available.

Synthesis of Half-Titanocene Complexes

Synthesis of Compounds 1a–f

Various *o*-di(phenyl)phosphanylphenol ligands bearing different substituents on R^1 and R^2 positions, 2-R^1-4-R^2-6-$(PPh_2)C_6H_2OH$ (**1a**: $R^1 = R^2 = H$; **1b**: $R^1 = F$, $R^2 = H$; **1c**: $R^1 = Ph$, $R^2 = H$; **1d**: $R^1 = SiMe_3$, $R^2 = H$; **1e**: $R^1 = {}^t$Bu, $R^2 = H$; **1f**: $R^1 = R^2 = {}^t$Bu) were prepared according to literature procedures.[19,22]

Synthesis of Half-titanocene Complexes 2a–f

Half-titanocene complexes **2a–f** were synthesized according to literature procedures.[19] Complex **2a** was obtained as orange red crystals in 70% yield. ^{1}H NMR (300 MHz, $CDCl_3$, 298 K): δ 7.43–7.28 (m, 11H, Ar-H), 7.04–6.97 (m, 2H, Ar-H), 6.78 (ddd, J = 7.8, 4.0, 1.5 Hz, 1H, Ar-H), 6.50 (s, 5H, C_5H_5). ^{13}C NMR (151 MHz, $CDCl_3$, 298 K): δ 170.03 (d, J = 19.6 Hz), 135.45 (d, J = 7.2 Hz), 134.26 (d, J = 19.4 Hz), 133.22, 130.79, 129.39, 128.80 (d, J = 7.3 Hz), 127.31 (d, J = 9.4 Hz), 124.34, 121.28, 120.17. ^{31}P NMR (121.5 MHz, $CDCl_3$, 298 K): δ −14.91 ppm. Anal. Calc. For $C_{23}H_{19}Cl_2OPTi$: C, 59.90; H, 4.15. Found: C, 59.72; H, 4.08.

Complex **2b** was obtained as orange crystals in 65% yield. ^{1}H NMR (300 MHz, $CDCl_3$, 298 K): δ 7.44–7.28 (m, 11H, Ar-H), 7.18–7.09 (m, 1H, Ar-H), 6.90 (td, J = 7.3, 4.8 Hz, 1H, Ar-H), 6.48 (s, 5H, C_5H_5). ^{13}C NMR (151 MHz, $CDCl_3$, 298 K): δ 157.27 (dd, J = 20.0), 153.90 (d, J = 254.0 Hz), 135.20 (d, J = 9.7 Hz), 134.44 (d, J = 20.2 Hz), 131.47 (d, J = 14.7 Hz), 129.47, 128.80 (d, J = 7.2 Hz), 128.14, 123.89 (d, J = 6.5 Hz), 121.78, 117.08 (d, J = 18.7 Hz). ^{31}P NMR (121.5 MHz, $CDCl_3$, 298 K): δ −17.10 ppm. Anal. Calc. For $C_{23}H_{18}Cl_2FOPTi$: C, 57.66; H, 3.79. Found: C, 57.42; H, 3.71.

Complex **2c** was obtained as orange crystals in 72% yield. ^{1}H NMR (300 MHz, $CDCl_3$, 298 K): δ 7.61–7.57 (m, 2H, Ar-H), 7.51–7.34 (m, 14H, Ar-H), 7.07 (t, J = 7.5 Hz, 1H, Ar-H), 6.84 (ddd, J = 7.6, 3.9, 1.6 Hz, 1H, Ar-H), 5.97 (s, 5H, C_5H_5). ^{13}C NMR (151 MHz, $CDCl_3$, 298 K): δ 168.42 (d, J = 21.4 Hz), 137.28, 135.49, 134.13 (d, J = 17.8 Hz, 81H), 133.14, 132.59, 132.00, 130.60, 129.50, 128.86, 128.80, 128.75, 127.64, 124.00, 121.37. ^{31}P NMR (121.5 MHz, $CDCl_3$, 298 K): δ −10.54 ppm. Anal. Calc. For $C_{29}H_{23}Cl_2OPTi$: C, 64.83; H, 4.32. Found: C, 64.91; H, 4.38.

Complex **2d** was obtained as orange red crystals in 78% yield. ^{1}H NMR (300 MHz, $CDCl_3$, 298 K): δ 7.76–7.64 (m, 4H, Ar-H), 7.49 (m, 7H, Ar-H) 7.41–7.34 (m, 1H, Ar-H), 6.98 (t, J = 7.3 Hz, 1H, Ar-H), 6.44 (d, J_{HP} = 2.6 Hz, 5H, C_5H_5), 0.37 (s, 9H, $Si(CH_3)_3$). ^{13}C NMR (151 MHz, $CDCl_3$, 298 K): δ 177.23 (d, J = 27.0 Hz), 139.39, 134.18, 132.52 (d, J = 9.5 Hz), 131.12, 129.28 (d, J = 9.5 Hz), 128.61, 123.09, 122.82, 121.83, 121.28, −0.99. ^{31}P NMR (121.5 MHz, $CDCl_3$, 298 K): δ 25.42 ppm. Anal. Calc. For $C_{26}H_{27}Cl_2OPSiTi$: C, 58.55; H, 5.10. Found: C, 58.41; H, 5.03.

Complex **2e** was obtained as red crystals in 87% yield. ^{1}H NMR (300 MHz, $CDCl_3$, 298 K): δ 7.76–7.64 (m, 4H, Ar-H), 7.49 (m, 6H, Ar-H), 7.38 (d, J = 7.7 Hz, 1H, Ar-H), 7.25–7.19 (m, 1H, Ar-H), 6.93 (td, J = 7.6, 1.5 Hz, 1H, Ar-H), 6.44 (d, J_{HP} = 2.6 Hz, 5H, C_5H_5), 1.45 (s, 9H, ^{t}Bu-H). ^{13}C NMR (151 MHz, $CDCl_3$, 298 K): δ 171.16 (d, J = 27.4 Hz), 138.53 (d, J = 4.2 Hz), 132.51 (d, J = 9.3 Hz), 131.10, 130.94, 130.79, 129.25 (d, J = 9.4 Hz), 125.21, 124.92, 122.18 (d, J = 5.2 Hz), 121.21, 35.26, 29.73. ^{31}P NMR (121.5 MHz, $CDCl_3$, 298 K): δ 27.18 ppm. Anal. Calc. For $C_{27}H_{27}Cl_2OPTi$: C, 62.69; H, 5.26. Found: C, 62.58; H, 5.20.

Complex **2f** was obtained as red crystals in 80% yield. ^{1}H NMR (300 MHz, $CDCl_3$, 298 K): δ 7.74–7.64 (m, 4H, Ar-H), 7.49 (m, 6H, Ar-H), 7.40 (d, J = 2.1 Hz, 1H, Ar-H), 7.17 (dd, J = 6.4, 2.2 Hz, 1H, Ar-H), 6.43 (d, J_{HP} = 2.6 Hz, 5H, C_5H_5), 1.45 (s, 9H, ^{t}Bu-H), 1.26 (s, 9H, ^{t}Bu-H). ^{13}C NMR (151 MHz, $CDCl_3$, 298 K): δ 169.29 (d, J = 27.6 Hz), 144.79 (d, J = 4.5 Hz), 137.14 (d, J = 4.5 Hz), 132.54 (d, J = 9.3 Hz), 130.94, 129.17 (d, J = 9.3 Hz), 128.16, 127.33, 124.35, 124.06, 121.11, 35.38, 34.71, 31.61, 29.82. ^{31}P NMR (121.5 MHz, $CDCl_3$, 298 K): δ 26.99 ppm. Anal. Calc. For $C_{31}H_{35}Cl_2OPTi$: C, 64.94; H, 6.15. Found: C, 64.87; H, 6.10.

Copolymerization of Ethylene with Norbornene

A typical procedure was performed as follows: the prescribed amounts of toluene, NBE and cocatalyst were added into the autoclave (100 mL, stainless steel), and the apparatus was then purged with ethylene. The reaction mixture was then pressurized to the prescribed ethylene pressure soon after the addition of a toluene solution containing titanium complex. The polymerization was terminated with the addition of EtOH, and the resultant polymer was adequately washed with EtOH containing HCl and then dried under vacuum for several hours. The polymerization of ethylene was also performed in the same manner in the absence of NBE.

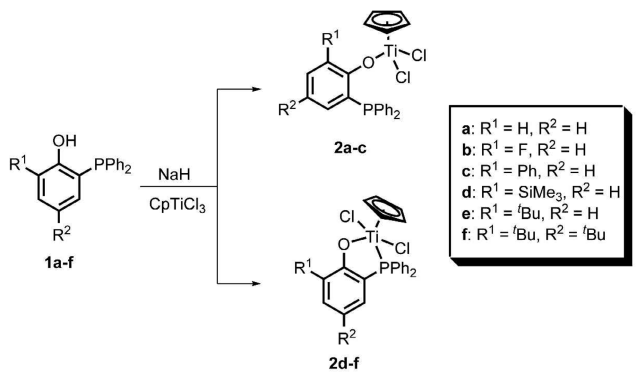

SCHEME 1 Synthesis of complexes **2a–f**.

Crystallographic Studies

Single crystals of complexes **2c–f** suitable for X-ray structure determination were grown from the chilled concentrated mixture of dichloromethane and hexane solution at −30 °C in a glove box, thus maintaining a dry, O_2-free environment. The intensity data were collected with the ω scan mode (186 K) on a Bruker Smart APEX diffractometer with CCD detector using Mo Kα radiation (λ = 0.71073 Å). Lorentz, polarization factors were made for the intensity data and absorption corrections were performed using SADABS program. The crystal structures were solved using the SHELXTL program and refined using full matrix least squares. The positions of hydrogen atoms were calculated theoretically and included in the final cycles of refinement in a riding model along with attached carbons.

Density Functional Theory Calculations

Density functional theory (DFT) calculations were used for the mechanism of copolymerization of ethylene and NBE with complex **2a** by using the Amsterdam Density Functional program package.[23] Geometry optimizations and energy calculations were performed using the local density approximation augmented with Becke's nonlocal exchange corrections and Perdew's nonlocal correction.[24,25] A triple STO basis set was used for Ti, whereas all other atoms were described by a double-ζ plus polarization STO basis. The 1s electrons of the C, P, and O atoms, as well as the 1s-2p electrons of Ti atom, were treated as frozen core. Finally, first-order scalar relativistic corrections were added to the total energy of the system.

RESULTS AND DISCUSSION

Synthesis and Structural Analysis of Complexes $CpTiCl_2[O\text{-}2\text{-}R^1\text{-}4\text{-}R^2\text{-}6\text{-}(Ph_2P)C_6H_2]$

Titanium complexes **2a–f** have been prepared in high yields (65–87%) by treating $CpTiCl_3$ with 1.0 equiv of the sodium salts of *o*-di(phenyl)phosphanylphenols, which were prepared by the corresponding ligands with NaH, as shown in Scheme 1.

Pure samples were collected from the chilled concentrated mixture of dichloromethane and hexane solution placed in the freezer (−30 °C). The resultant complexes were identified by ^{1}H, ^{13}C, and ^{31}P NMR spectra and elemental analyses. The ^{1}H NMR spectra of these complexes showed no complexity, and the integration of complexes confirms a 1:1 ratio of cyclopentadienyl to *o*-di(phenyl)phosphanylphenolate ligand. A sharp single resonance at δ 5.97–6.50 ppm assigned to the C_5H_5(Cp) protons were observed in complexes **2a–c** (**2a**, δ 6.50 ppm; **2b**, δ 6.48 ppm; **2c**, δ 5.97 ppm), whereas the ^{1}H NMR spectra of **2d–f** display a doublet for the Cp hydrogens (**2d**, δ 6.44 ppm, J_{HP} = 2.6 Hz; **2e**, δ 6.44 ppm, J_{HP} = 2.6 Hz; **2f**, δ 6.43 ppm, J_{HP} = 2.6 Hz) suggesting phosphorus is coordinated to titanium. In addition, the configurations of **2a–f** in solution were also determined by ^{31}P NMR spectroscopy. All signals in the ^{31}P NMR spectra were shifted substantially downfield from the values found for the corresponding ligands. Note that the values of **2d–f** (**2d**, δ 25.42 ppm; **2e**, δ 27.18 ppm; **2f**, δ 26.99 ppm) are consistent with a triarylphosphine bound to a metal center.[19] However, the chemical shifts of **2a–c** (**2a**, δ −14.91 ppm; **2b**, δ −17.10 ppm; **2c**, δ −10.54 ppm) were at higher field than **2d–f**, which indicates that the phosphorus is not coordinated to Ti.

Crystals of **2c–f** suitable for crystallographic analysis were grown from the chilled concentrated CH_2Cl_2-hexane mixture solution. The crystallographic data together with the collection and refinement parameters are summarized in Table 1. Selected bond distances and angles for **2c–f** were summarized in Table 2. If the centroid of the cyclopentadienyl ring is considered as a single coordination site, complex **2c** (Fig. 1) is the pseudo tetrahedral geometry about the metal atom, and the phosphorus is not coordinated. However, complexes **2d–f** adopt five-coordinate, distorted square–pyramid geometry around the titanium center, in which the equatorial positions are occupied by oxygen and phosphorus atoms of the ligands and two chlorine atoms. The cyclopentadienyl group is coordinated on the axial position, as shown in Figures 2 and 3 and Supporting Information Figure S1. The configurations of **2c–f** in the solid state were in line with the results observed in the ^{31}P NMR spectra. These results clearly indicate that the steric bulk in R^1 position appears to be required in generation of five-coordinate, distorted square–pyramid geometry around the titanium center.

Complex **2c** closely resembles the structure of other cyclopentadienyl phenoxide complexes with bulky ortho-substituents rather than the five-coordinate complexes **2d–f**. For example, the Ti(1)—O(1) bond distance in **2c** [1.795 (2) Å] is shorter than those in **2d–f** [**2d**: 1.8708 (13), **2e**: 1.872 (3), **2f**: 1.8751 (18) Å), but is close to that in $CpTiCl_2$ (2-Ph-4,6-^{t}Bu$_2$C$_6$H$_2$O) [1.785 (2) Å] and Cp*TiCl$_2$(O-2,6-Me$_2$C$_6$H$_3$) [1.785 (2) Å].[26] Ti-Cp (centroid) distances in **2d–f** (**2d**: 2.034, **2e**: 2.031, **2f**: 2.036 Å) are somewhat longer than that in **2c** (2.016 Å), but shorter than that in $CpTiCl_2$[O-2-^{t}Bu-6-(Ph$_2$P=O)C$_6$H$_2$] (**3a**, 2.043 Å).[17(b)] The distance between Ti(1) and P(1) in **2c** is 4.073 Å, suggesting that the phosphorus atom is not coordinated to the metal center in the solid state. The five-membered C_2OPTi chelate ring in **2d–f** has an envelope conformation with the metal lying about 0.549–0.603 Å (**2d**: 0.549, **2e**: 0.603, **2f**: 0.593 Å) out of the C_2OP plane in the direction of Cp ring. The Ti(1)—P(1) bond length in **2d–f** is obviously affected by the R^1 and R^2 groups

TABLE 1 Crystal Data and Structure Refinements of Complexes 2c–f

	2c	2d	2e	2f
Empirical formula	$C_{29}H_{23}Cl_2OPTi$	$C_{27}H_{29}Cl_4OPSiTi$	$C_{28}H_{29}Cl_4OPTi$	$C_{32}H_{37}Cl_4OPTi$
Formula weight	537.24	618.26	602.18	658.26
Crystal system	Monoclinic	Triclinic	Triclinic	Triclinic
Space group	P2 (1)/*n*	P-1	P-1	P-1
a (Å)	11.2213 (10)	10.0885 (5)	10.0569 (7)	9.9008 (10)
b (Å)	19.6800 (18)	10.5105 (5)	10.3311 (7)	13.4317 (14)
c (Å)	12.0674 (11)	14.8640 (7)	16.2854 (11)	13.8494 (14)
α (°)	90.00	84.4960 (10)	106.0040 (10)	100.981 (2)
β (°)	109.550 (2)	74.6440 (10)	92.4440 (10)	103.992 (2)
γ (°)	90.00	70.91	118.2480 (10)	106.771 (2)
V (Å^3), *Z*	2,511.3 (4), 4	1,436.18 (12), 2	1,402.49 (17), 2	1,642.6 (3), 2
$Density_{calcd}$ (Mg/m^3)	1.421	1.430	1.426	1.331
Absorption coefficient (mm^{-1})	0.638	0.787	0.764	0.658
F(000)	1,104	636	620	684
Crystal size (mm)	0.26 × 0.20 × 0.14	0.32 × 0.26 × 0.18	0.36 × 0.29 × 0.20	0.36 × 0.28 × 0.24
θ range for data collection (°)	2.07–25.32	1.42–26.11	2.30–26.11	1.96–25.09
Reflections collected	12,729	8,054	7,864	8,471
Independent reflections	4,559 (R_{int} = 0.0602)	5,633 (R_{int} = 0.0127)	5,475 (R_{int} = 0.0242)	5,766 (R_{int} = 0.0229)
Data/restraints/parameters	4,559/0/307	5,633/0/319	5,475/0/316	5,766/0/352
Goodness-of-fit on F^2	1.037	1.035	1.058	1.072
Final *R* indices [$I > 2\sigma(I)$]: R^1, wR^2	0.0491, 0.1118	0.0316, 0.0811	0.0636, 0.1533	0.0437, 0.1086
Largest diff. peak and hole (e/Å^3)	0.387 and −0.440	0.432 and −0.322	1.534 and −1.325	0.594 and −0.592

TABLE 2 Selected Bond Distances (Å) and Angles (°) for Complexes 2c–f

	2c	2d	2e	2f
		Bond distances (Å)		
Ti(1)—O(1)	1.795 (2)	1.8708 (13)	1.872 (3)	1.8751 (18)
Ti(1)—P(1)		2.6446 (6)	2.6208 (12)	2.6285 (8)
Ti(1)—Cl(1)	2.2582 (11)	2.3320 (6)	2.3435 (12)	2.3297 (8)
Ti(1)—Cl(2)	2.2478 (11)	2.3453 (6)	2.3376 (12)	2.3291 (7)
Ti(1)-Cp(centroid)	2.016	2.034	2.031	2.036
O(1)—C(1)	1.369 (4)	1.360 (2)	1.354 (5)	1.353 (3)
P(1)—C(2)	1.835 (3)	1.7994 (19)	1.804 (4)	1.801 (3)
		Bond angles (°)		
Cl(1)—Ti(1)—Cl(2)	101.45 (4)	88.96 (2)	88.84 (5)	88.70 (3)
O(1)—Ti(1)—P(1)		72.85 (4)	72.28 (8)	72.45 (5)
Ti (1)—O(1)—C(1)	161.39 (19)	134.99 (11)	135.5 (2)	135.31 (15)
Ti (1)—P(1)—C(2)		97.11 (6)	97.45 (13)	97.24 (9)
Cl(1)—Ti(1)—O(1)	104.48 (7)	127.96 (5)	129.66 (9)	129.25 (6)
Cl(2)—Ti(1)—O(1)	103.92 (7)	90.17 (4)	89.28 (9)	88.73 (6)
Cl(1)—Ti(1)—P(1)		78.40 (2)	79.61 (4)	80.38 (3)
Cl(2)—Ti(1)—P(1)		144.48 (2)	142.81 (4)	143.53 (3)
O(1)—C(1)—C(2)	117.8 (3)	118.22 (16)	117.3 (3)	117.5 (2)
P(1)—C(2)—C(1)	117.7 (2)	111.70 (14)	111.2 (3)	111.48 (19)

of the ligand [**2d**: 2.6446 (6), **2e**: 2.6208 (12), **2f**: 2.6285 (8) Å]. The Ti(1)—P(1) bond distances in **2d–f** appear in the range of 2.6208–2.6446 Å, indicative of significant coordination of phosphorus atom to the metal center in the solid state. However, the Ti(1)—O(1), O(1)—C(1), and P(1)—C(2) bond lengths in **2d–f** change slightly with the variation in R^1 and R^2 groups, as shown in Table 2. The two Ti(1)—Cl bond lengths in **2e–f** are statistically identical [**2e**: 2.3435 (12) and 2.3376 (12) Å, **2f**: 2.3297 (8), and 2.3291 (7) Å to Cl(1) and Cl(2), respectively], whereas in **2c–d** the two Ti(1)—Cl bond lengths are noticeably different [**2c**: 2.2582 (11) and 2.2478 (11) Å, **2d**: 2.3320 (6) and 2.3453 (6) Å to Cl(1) and Cl(2), respectively]. The bond angles for Cl(1)—Ti(1)—Cl(2) in **2d–f** [**2d**: 88.96 (2)°, **2e**: 88.84 (5)°, **2f**: 88.70 (3)°, respectively] are smaller than that for complex **2c** [101.45 (4)°], but larger than that for complex **3a** [84.955 (19)°].[17(b)] Moreover, the bond distances and angles for **2d** are consistent with those reported previously.[19]

Ethylene (Co)polymerization Catalyzed by 2a–f

Ethylene polymerizations by $CpTiCl_2[2\text{-}R^1\text{-}4\text{-}R^2\text{-}6\text{-}PPh_2\text{-}C_6H_2O]$ (**2a–f**) in the presence of MMAO were examined to explore the effect of the steric environments near the metal center on the catalytic activity. Complex **2a** showed moderate catalytic activity (**2a**, 380 kg/mol$_{Ti}$ h) for ethylene polymerization (conditions: 5.0 μmol catalyst, ethylene 4 atm,

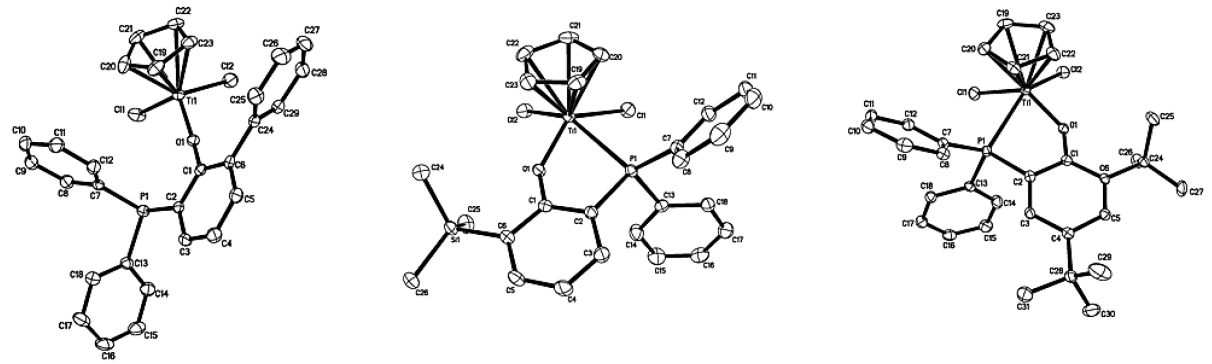

FIGURE 1 ORTEP drawings for $CpTiCl_2[O\text{-}2\text{-}R^1\text{-}4\text{-}R^2\text{-}6\text{-}(Ph_2P)C_6H_2]$ [R^1 = Ph, R^2 = H (**2c**, left); R^1 = $SiMe_3$, R^2 = H (**2d**, middle); R^1 = R^2 = ^{t}Bu (**2f**, right)]. Thermal ellipsoids are drawn at the 30% probability level. H atoms and the solvent molecule are omitted for clarity.

MMAO/Ti = 1000, 20°C, 10min, V_{total} = 50 mL). Introducing electron-withdrawing group or electron-donating group in R^1 position decreased the activity (**2b**: 220 kg/mol$_{Ti}$ h, **2c**: 290 kg/mol$_{Ti}$ h, **2d**: 160 kg/mol$_{Ti}$ h, **2e**: 200 kg/mol$_{Ti}$ h, **2f**: 130 kg/mol$_{Ti}$ h, respectively). Complex **2f**, bearing *tert*-butyl groups in both R^1 and R^2 position, exhibited lowest activities among these catalysts, in complete contrast to the results by $CpTiCl_2[2\text{-}R^1\text{-}4\text{-}R^2\text{-}6\text{-}P(=O)Ph_2\text{-}C_6H_2O]$, among which complex bearing *tert*-butyl groups in both R^1 and R^2 position exhibited the highest activity.[17(b)]

$Ph_3CB(C_6F_5)_4/^iBu_3Al$ is also effective cocatalyst for olefin polymerization.[27] Fujita et. al. reported that bis[*N*-(3-*tert*-butylsalicylidene)-anilinato]zirconium(IV) dichloride activated with $Ph_3CB(C_6F_5)_4/^iBu_3Al$ gave extremely high molecular weight polyethylene. This complex in combination with $Ph_3CB(C_6F_5)_4/^iBu_3Al$ could provide a high molecular weight ethylene-propylene copolymer, Mv 109 × 10^4, with 8000 kg of polymer/mol of cat·h activity at a propylene content of 20.7 mol %.[28] Our recent research indicated that $CpZrCl_2[O\text{-}2R_1\text{-}4R_2\text{-}6(Ph_2P{=}O)C_6H_2]$ in combination with $Ph_3CB(C_6F_5)_4/^iBu_3Al$ generated high molecular weight polymer with high efficiency.[17(b)] Therefore, herein, we also explored ethylene/NBE copolymerization using $Ph_3CB(C_6F_5)_4/i\text{-}Bu_3Al$ as cocatalyst. In the presence of $Ph_3CB(C_6F_5)_4/^iBu_3Al$, complexes **2a–f** only produced trace polymers for ethylene polymerization under the similar conditions (conditions: 5.0-μmol catalyst, ethylene 4 atm, 20 °C, 10min, [Al]/[B]/[Ti] = 100/2/1, V_{total} = 50 mL). Surprisingly, notable improvements in the catalytic activity were observed if introducing NBE into the reaction system, in complete contrast to the results of the copolymerization by bridged metallocene and linked half-titanocene reported previously,[29,30] in which the catalytic activity decreased upon increasing the NBE concentration. The copolymerization by **2a**/$Ph_3CB(C_6F_5)_4/^iBu_3Al$ catalyst system also took place, and the observed activity calculated on the basis of the polymer yield was twice higher than that by **2a**/MMAO system (5.0-μmol catalyst, $[NBE]_{initial}$ = 0.5 mol/L, **2a**/MMAO: 1660 kg/mol$_{Ti}$·h; **2a**/$Ph_3CB(C_6F_5)_4/^iBu_3Al$: 3300 kg/mol$_{Ti}$·h**)**. Because of better performance observed by $Ph_3CB(C_6F_5)_4/^iBu_3Al$ as the cocatalyst, E/NBE copolymerizations by **2a–f** were investigated in

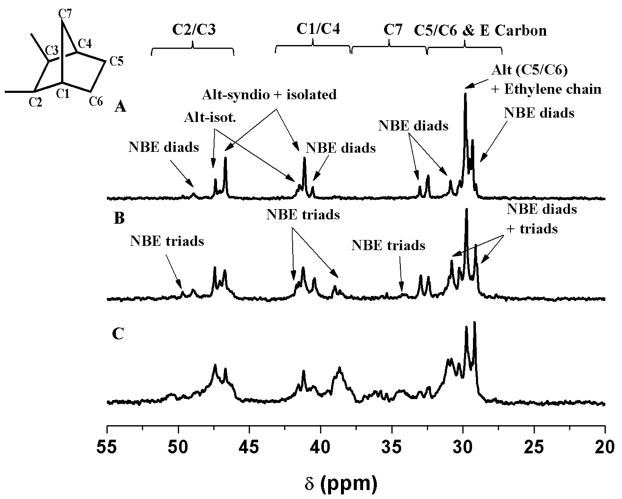

FIGURE 2 ^{13}C NMR spectra of E/NBE copolymer with different NBE incorporations produced by **2d** (A: 27.2%, entry 7; B: 51.7%, entry 8; C: 67.8%, entry 16 in Table 3, respectively).

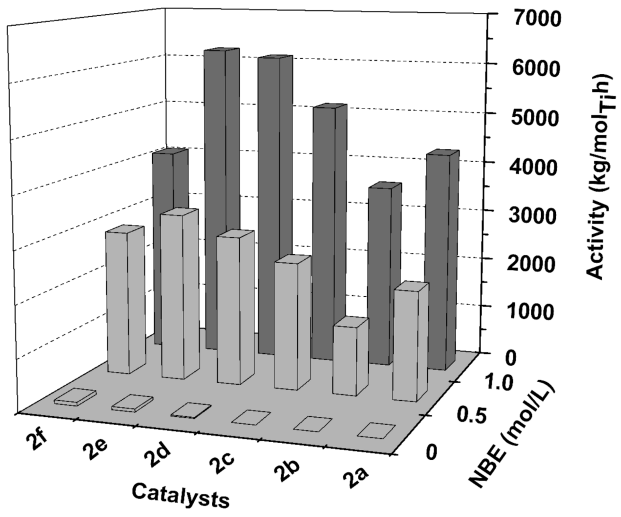

FIGURE 3 Catalytic activities of the complexes **2a–f** toward ethylene (co)polymerization at different NBE concentrations.

TABLE 3 Copolymerization of Ethylene with NBE by **2a–f**[a]

Entries	Catalyst (μmol)	*E* (atm)	Temperature (°C)	Time (min)	NBE (mol/L)	Yield (mg)	Activity (kg/mol$_{Ti}$ h)	M_w[b] (10^{-4})	M_w/M_n[b]	NBE Incorporation (%)[c]
1	**2a** (1.0)	4	20	10	0.5	350	2,100	22.8	2.4	28.1
2	**2a** (1.0)	4	20	5	1.0	360	4,320	14.6	2.2	53.2
3	**2b** (1.0)	4	20	10	0.5	220	1,320	14.7	2.3	26.4
4	**2b** (1.0)	4	20	5	1.0	300	3,600	11.5	2.1	43.0
5	**2c** (1.0)	4	20	10	0.5	410	2,460	Bimodal		
6	**2c** (1.0)	4	20	5	1.0	430	5,160	Bimodal		
7	**2d** (1.0)	4	20	10	0.5	480	2,880	12.6	2.3	27.2
8	**2d** (1.0)	4	20	5	1.0	510	6,120	14.5	2.2	51.7
9	**2e** (1.0)	4	20	10	0.5	540	3,240	16.1	2.5	22.6
10	**2e** (1.0)	4	20	5	1.0	520	6,240	11.1	2.1	35.8
11	**2f** (1.0)	4	20	10	0.5	470	2,820	14.1	2.3	26.0
12	**2f** (1.0)	4	20	5	1.0	340	4,080	12.2	2.2	44.7
13[d]	**2d** (1.0)	4	20	5	1.0	460	5,520	13.8	2.2	50.4
14	**2d** (1.0)	4	40	5	1.0	400	4,800	10.0	2.1	53.2
15	**2d** (1.0)	2	20	10	1.0	350	2,100	9.8	2.3	56.3
16	**2d** (5.0)	1	20	10	1.0	150	180	3.8	2.2	67.8
17	**2d** (1.0)	4	20	5	2.0	180	2,160	16.2	2.1	59.4

[a] Conditions: $Ph_3CB(C_6F_5)_4$/$^iBu_3Al$ as the cocatalyst, [Al]/[B]/[Ti] = 100/2/1, V_{total} = 50 mL; [b] Weight-average molecular weights and polydispersity indices determined by high temperature GPC at 150 °C in 1,2,4-$C_6Cl_3H_3$ versus narrow polystyrene standards; [c] NBE content (mol %) estimated by ^{13}C NMR spectra; [d] [Al]/[B]/[Ti] = 200/2/1.

detail in the presence of $Ph_3CB(C_6F_5)_4$/$^iBu_3Al$. Polymerization conditions such as catalyst concentration and polymerization time were varied in order to control the NBE conversion ($< \sim$10%). The results of the copolymerization are shown in Table 3 together with the molecular weights and molecular weight distributions as well as NBE incorporation of the resultant copolymers.

It was revealed that **2a** exhibited both high catalytic activity and efficient NBE incorporation. The observed catalytic activities and NBE incorporations enhanced upon increasing the NBE concentration in feed from 0.5 to 1.0 mol/L. The resultant copolymers possessed relatively high MWs with unimodal molecular weight distributions (MWDs), and the MW values for the copolymers decreased upon increasing NBE contents (entries 1–2). Both the observed activities and NBE incorporation by **2b** were lower than those by **2a** in ethylene/NBE copolymerization under the same conditions (entries 3–4). Analog **2c** had comparable structures with **2a** and **2b**, but it produced bimodal MWDs polymers under the same conditions (entries 5–6). There appears no clear reason at this moment why **2c** afforded poly(E-*co*-ENB)s with bimodal MWDs. One possible explanation is that the conjugated phenyl group in R^1 position is much unfavored for stabilizing the active species. Complex **2d** was found to display a very high activity of 6120 kg/mol$_{Ti}$ h at high NBE concentration, which was about 150 times larger than that of ethylene homopolymerization. Moreover, **2d** showed higher NBE incorporation than **2b**, and the efficiency is at the same level as that by **2a**. The MWs of the resultant copolymers by **2d** increased on increasing NBE concentration, whereas the MW values by the other catalysts decreased on increasing the NBE concentration. Analog **2e** also exhibited remarkable catalytic activity, but less NBE incorporation than **2d** under the same conditions (entries 9–10). The NBE contents in the resultant copolymers by **2f** were similar to those obtained by **2b** under the same conditions (entries 11–12). Therefore, analog **2d** should be the most suited catalyst precursor for the ethylene/NBE copolymerization in terms of both catalytic activity and NBE incorporation.

We used catalyst **2d** to explore the effect of various reaction parameters like Al/Ti molar ratio, reaction temperature and ethylene pressure on copolymerization behaviors. As summarized in Table 3, the increase in Al/Ti molar ratio caused significant change neither in the catalytic activity nor the MWs for the resultant poly(ethylene-*co*-NBE)s (entries 13 vs. 8). In addition, NBE incorporation was also independent of the Al/Ti molar ratio. These results suggest that the dominant chain-transfer pathway is not chain-transfer to aluminum alkyls but seems to be β-hydrogen transfer under these conditions. Both the activity and the MW decreased when the copolymerization was conducted at the higher temperature of 40 °C (entry 14). The efficient syntheses of the copolymers with high NBE contents (50–70 mol %) could be accomplished upon increasing the NBE concentration or decreasing low ethylene pressure (entries 8, 15–16). Although the observed catalytic activities enhanced upon increasing the NBE concentration, the activity decreased gradually at higher NBE concentration conditions (entry 17).

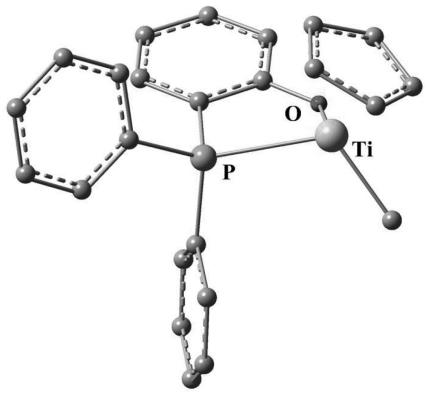

FIGURE 4 Assumed catalytically active species, the optimized structure of **1**.

An extremely low activity was observed (activity $<$ 1 kg/mol_{Ti} h) when the polymerization was performed in the absence of ethylene.

The typical ^{13}C NMR spectra of poly(ethylene-*co*-NBE)s with different NBE incorporations are illustrated in Figure 4.[29–32] Figure 4(A) shows that the microstructures of the COCs formed using **2d** under low NBE concentration of 0.5 mol/L possessed few NBE repeat units and contained alternating ethylene-NBE sequences as well as isolated NBE units. In contrast, resonances ascribed to NBE diads or triads were observed for the copolymers prepared at high NBE concentration of 1.0 mol/L and/or under low ethylene pressure [Fig. 4(B,C)], and the microstructures thus possessed a mixture of NBE repeat units in addition to the alternating, isolated NBE sequences.

Theoretical Calculations

Complexes **2a–c** and **2d–f** possessed different configurations in the solid state. A question arises: why they could display similar behaviors in ethylene/NBE copolymerization? Moreover, complexes **2a–f** could effectively promote neither ethylene polymerization nor NBE polymerization in the presence of $Ph_3CB(C_6F_5)_4/{}^iBu_3Al$, why these complexes displayed notable activities in ethylene/NBE copolymerization (Fig. 3)?

Attempt to alkylate above complexes was unsuccessful, some unidentified products was obtained. As well known, quantum chemical analysis has become a very powerful tool for predicting the structures of catalytically active species before the actual experimental proof. Therefore, we chose four-coordinate complex **2a** and five-coordinate complex **2d** to explore their active forms, $CpTiMe[O\text{-}6\text{-}(Ph_2P)C_6H_3]^+$ and $CpTiMe[O\text{-}2\text{-}{}^tBu\text{-}6\text{-}(Ph_2P)C_6H_3]^+$, based on DFT calculations. The conformation with the lowest energy was chosen as the final model. The computed ground state arrangement of the $CpTiMe[O\text{-}2\text{-}{}^tBu\text{-}6\text{-}(Ph_2P)C_6H_3]^+$ has a pseudotetrahedral geometry around the Ti center. Unexpectedly, $CpTiMe[O\text{-}6\text{-}(Ph_2P)C_6H_3]^+$ also adopted pseudotetrahedral geometry to Ti, meaning that the phosphorus is coordinated to Ti in the case of the cationic active species, as shown in Figure 4. It seems likely, therefore, that two unpaired electrons of phosphorus were pushed back to the electron-deficient metal center resulting in the formation the 12-electron, cationic metal alkyl species (**1**). In this way, π-type interaction between the Ti atom and the P atom could help to stabilize the species. This should be conveniently observed in the ^{31}P NMR spectra for the changed phosphorus environments. The ^{31}P NMR spectrum of **2e** showed a single ^{31}P resonance at 19.5 ppm in the presence of $Ph_3CB(C_6F_5)_4/{}^iBu_3Al$. Note that a resonance at 21.3 ppm also appeared in ^{31}P spectrum of **2a** in the presence of $Ph_3CB(C_6F_5)_4/{}^iBu_3Al$, apparently indicating the phosphorus is coordinated to titanium in the catalytically active species. Introducing ethylene and NBE into the catalyst systems afforded the resonances in the ^{31}P NMR spectra in the range of 16.6–21.3 ppm for **2e** and 16.5–25.3 ppm for **2a**. Therefore, we assumed that these complexes possess similar cationic active species, which also provided a suitable rationale for **2a–f** displaying similar behaviors in ethylene (co)polymerization.

Based on the above results, reaction energies were calculated using complex $CpTiMe[O\text{-}6\text{-}(Ph_2P)C_6H_4]^+$ (**1**) as model. Reaction energy profiles were obtained by following the well-established Cossée–Arlman or Brookhart–Green mechanism.[33] Our discussion has been built around the very first insertion step by modeling the growing chain end with a methyl group, corresponding to the initiation step in olefin polymerization. When the influence of the counterion is ignored, the insertion of monomer into the Ti—C bond of complex has usually been described as a two-step process: monomer uptake and insertion.[34–37] The uptake involves π-complexation of monomer to the metal center. The insertion goes through a transition state with a four-membered-ring structure.

Norbornene Competing with Ethylene

As shown in Figure 5, the complexation of NBE molecule to the Ti-alkyl cation lies 5.22 kcal/mol below the free Ti-alkyl cation and ethylene molecule (channel **b**), whereas ethylene complexation adduct is 1.36 kcal/mol below the baseline (channel **a**), indicating the complexation of NBE molecule to the cationic species is much easier. Compared to ethylene, NBE molecule can strengthen the C=C/Ti binding through an agostic hydrogen atom on the methylene bridge with the metal center, which accounts for much of the observed excess binding energy of NBE on complex **1**. The complex **2** not only is 3.86 kcal/mol less stable than the π-complex **5** but also lies in a shallow well, allowing for facile isomerization to the π-complex. In addition, the total barrier for channel **a** is 3.03 kcal/mol above the energy level of the reactants, while the barrier is reduced to -0.04 kcal/mol when NBE is introduced. Therefore, comparison of the two reaction channels **a** and **b** in Figure 7 shows that channel **b** is the preferred σ-bond metathesis channel.

To corroborate the result that channel **b** is favored, the rate constant ratio $k^{N\text{-}Me}/k^{E\text{-}Me}$ is calculated by the free energy change of the two monomers. The value of $k^{N\text{-}Me}/k^{E\text{-}Me}$ is 53, that is, NBE is more reactive than ethylene in this case. The formation of terminal adduct complexes **4** and **7** lies roughly 18 and 23 kcal/mol below the baseline, respectively. In

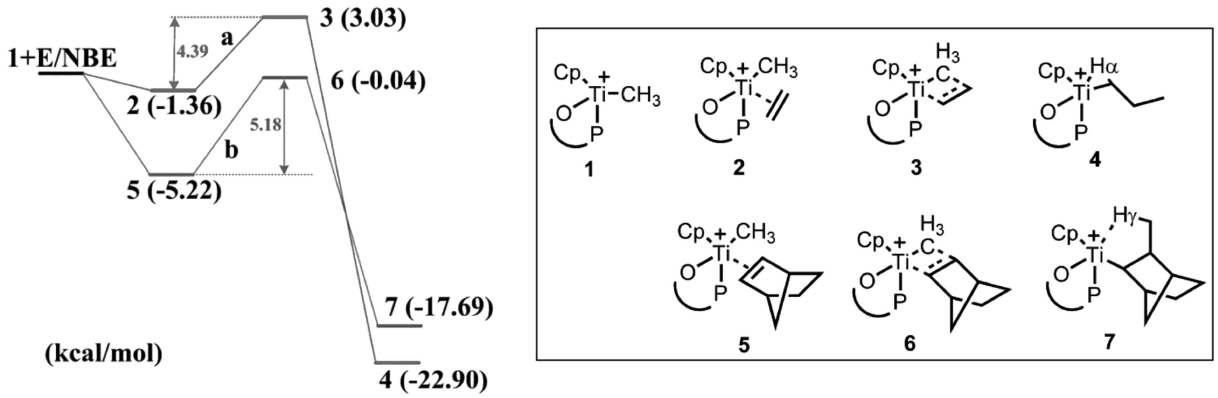

FIGURE 5 Schematic presentation of polymerization pathway.

addition, a hydrogen bound to the alkyl side chain is able to provide an additional agostic interaction to the metal in the transition state.

Chain End Effect

Although the model of the growing chain end with a methyl group can capture important aspects of the insertion mechanism beyond the very first event of monomer insertion, its applicability will be limited to a situation where the chain end consists of an ethylene or similar residue. Therefore, we show some results when the chain end is replaced by a NBE residue.

Our calculated energy profiles show that switching the chain end indeed raises the transition state of NBE well over that of ethylene (Fig. 6). Apparently, pathway **d** is preferred for the second ethylene propagation. The transition states are 1.61 kcal/mol lower in energy than the reactants, suggesting that ethylene insertion can easily take place in this case. Moreover, the rate constant ratio $k^{E\text{-}N}/k^{E\text{-}E}$ is about 3000. Therefore, it follows from our calculations as discussed above that NBE as a residue in the growing chain end is preferred over ethylene as residue for the chain propagation.

CONCLUSIONS

A series of *o*-di(phenyl)phosphanylphenolate-based half-titanocene complexes $CpTiCl_2[O\text{-}2\text{-}R^1\text{-}4\text{-}R^2\text{-}6\text{-}(Ph_2P)C_6H_2]$ (Cp = C_5H_5, **2a**: $R^1 = R^2 = H$; **2b**: $R^1 = F$, $R^2 = H$; **2c**: $R^1 = Ph$, $R^2 = H$; **2d**: $R^1 = SiMe_3$, $R^2 = H$; **2e**: $R^1 = {}^tBu$, $R^2 = H$; **2f**: $R^1 = R^2 = {}^tBu$) have been synthesized in high yields. The ^1H and ^{31}P NMR spectra indicated that the phosphorus is not coordinated to titanium in complexes **2a–c**, but is coordinated to Ti in complexes **2d–f**. Additionally molecular structures show that complex **2c** is essentially tetrahedral and the phosphorus is not coordinated, whereas complexes **2d–f** adopt five-coordinate distorted square–pyramid geometry around the titanium center. These novel titanium complexes showed moderate activity for ethylene polymerization, however they possessed excellent ability to copolymerize ethylene with NBE, affording the high molecular weight copolymers with high comonomer incorporations, especially in the case of $Ph_3CB(C_6F_5)_4/{}^iBu_3Al$ as cocatalyst.

Based on DFT calculations, the structures of cationic active species were predicted. Unexpectedly, these complexes possessed similar active species with pseudotetrahedral geometry around the Ti center. Furthermore, we identified that introducing NBE into the system not only can reduce the barrier of the transition state, but also are preferred for the second ethylene propagation. Thus, it seems that NBE does an amazing job in improving the catalytic activity, and even a small amount could accelerate polymerization process. The present catalyst system is thus a successful example for the efficient synthesis of random, high molecular weight copolymers with high NBE contents (>50 mol %). We believe that

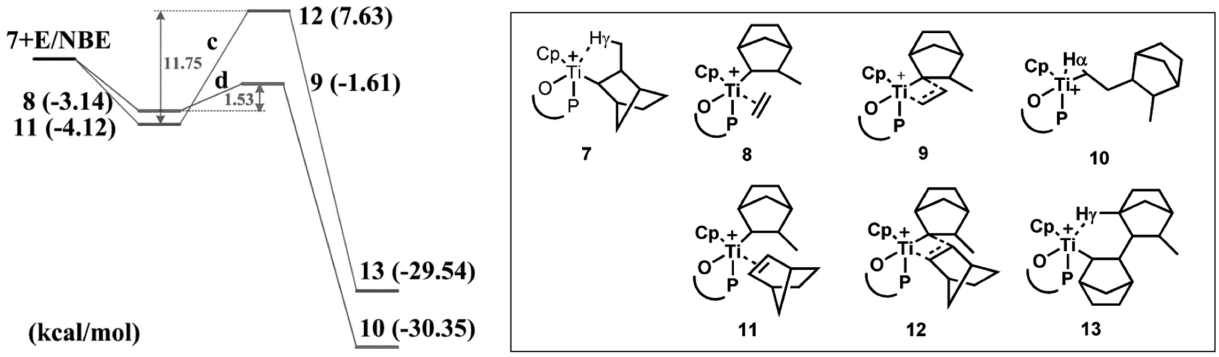

FIGURE 6 Schematic presentation of polymerization pathway.

the results through this study would introduce important information for designing efficient transition metal catalysts for the desired (co)polymerization.

ACKNOWLEDGMENTS

The authors are grateful for subsidy provided by the National Natural Science Foundation of China (Nos. 21074128 and 20923003). The authors also thank to Kotohiro Nomura (Tokyo Metropolitan University) for his discussion in preparing the manuscript.

REFERENCES AND NOTES

1 (a) K. Nomura, J. Y. Liu, S. Padmanabhan, B. Kitiyanan, *J. Mol. Catal. A: Chem.* **2007,** *267*, 1–29; (b) K. Nomura, *Dalton Trans.* **2009,** *38*, 8811–8823; (c) C. Redshaw, Y. Tang, *Chem. Soc. Rev.* **2012,** *41*, 4484–4510.

2 H. Sinn, W. Kaminsky, *Adv. Organomet. Chem.* **1980,** *18*, 99–105.

3 (a) D. W. Stephan, J. C. Stewart, F. Guerin, R. E. Spence, W. Xu, D. G. Harrison, *Organometallics* **1999,** *18*, 1116–1118; (b) F. Guerin, C. L. Beddie, D. W. Stephan, R. E. Spence, R. Wurz, *Organometallics* **2001,** *20*, 3466–3471; (c) D. W. Stephan, J. C. Stewart, F. Guerin, S. Courtenay, J. Kickham, E. Hollink, C. Beddie, A. Hoskin, T. Graham, P. R. Wei, R. E. V. Spence, W. Xu, L. Koch, X. L. Gao, D. G. Harrison, *Organometallics* **2003,** *22*, 1937–1947.

4 (a) K. Nomura, N. Naga, M. Miki, K. Yanagi, A. Imai, *Organometallics* **1998,** *17*, 2152–2154; (b) K. Nomura, N. Naga, M. Miki, K. Yanagi, *Macromolecules* **1998,** *31*, 7588–7597; (c) K. Nomura, K. Oya, T. Komatsu, Y. Imanishi, *Macromolecules* **2000,** *33*, 3187–3189; (d) K. Nomura, T. Komatsu, Y. Imanishi, *Macromolecules* **2000,** *33*, 8122–8124; (e) K. Nomura, H. Okumura, K. Komatsu, N. Naga, *Macromolecules* **2002,** *35*, 5388–5395; (f) K. Nomura, M. Tsubota, M. Fujiki, *Macromolecules* **2003,** *36*, 3797–3799; (g) K. Nomura, K. Fujki, *Macromolecules* **2003,** *36*, 2633–2641; (h) W. Wang, T. Tanaka, M. Tsubota, M. Fujiki, S. Yamanaka, K. Nomura, *Adv. Synth. Catal.* **2005,** *347*, 33–446.

5 M. K. Mahanthappa, A. P. Cole, R. M. Waymouth, *Organometallics* **2004,** *23*, 836–845.

6 A. Antiñolo, F. Carrillo-Hermosilla, A. Corrochano, J. Fernández-Baeza, A. Lara-Sanchez, M. R. Ribeiro, M. Lanfranchi, A. Otero, M. A. Pellinghelli, M. F. Portela, J. V. Santos, *Organometallics* **2000,** *19*, 2837–2843.

7 M. Tamm, S. Randoll, E. Herdtweck, N. Kleigrewe, G. Kehr, G. Erker, B. Rieger, *Dalton Trans.* **2006, 459–467.**

8 S. A. A. Shah, H. Dorn, A. Voigt, H. W. Roesky, E. Parisini, H. G. Schmidt, M. Noltemeyer, *Organometallics* **1996,** *15*, 3176–3181.

9 P. J. Sinnema, T. P. Spaniol, J. Okuda, *J. Organomet. Chem.* **2000,** *598*, 179–181.

10 W. P. Kretschmer, C. Dijkhuis, A. Meetsma, B. Hessen, J. H. Teuben, *Chem. Commun.* **2002, 608–609.**

11 S. B. Zhang, W. E. Piers, X. L. Gao, M. Parvez, *J. Am. Chem. Soc.* **2000,** *122*, 5499–5509.

12 (a) W. Zhang, L. R. Sita, *J. Am. Chem. Soc.* **2008,** *130*, 442–443; (b) W. Zhang, L. R. Sita, *Adv. Synth. Catal.* **2008,** *350*, 439–447; (c) K. C. Jayaratne, L. R. Sita, *J. Am. Chem. Soc.* **2000,** *122*, 958–959; (d) K. C. Jayaratne, R. J. Keaton, D. A. Henningsen, L. R. Sita, *J. Am. Chem. Soc.* **2000,** *122*, 10490–10491; (e) R. J. Keaton, K. C. Jayaratne, D. A. Henningsen, L. A. Koterwas, L. R. Sita, *J. Am. Chem. Soc.* **2001,** *123*, 6197–6198.

13 (a) R. Vollmerhaus, P. Shao, N. J. Taylor, S. Collins, *Organometallics* **1999,** *18*, 2731–2733; (b) S. Doherty, R. J. Errington, A. P. Jarvis, S. Collins, W. Clegg, M. R. J. Elsegood, *Organometallics* **1998,** *17*, 3408–3410.

14 (a) A. P. Dove, E. T. Kiesewetter, X. Ottenwaelder, R. M. Waymouth, *Organometallics* **2009,** *28*, 405–412; (b) A. P. Dove, X. Xie, R. M. Waymouth, *Chem. Commun.* **2005,** *16*, 2152–2154.

15 S. F. Liu, W. H. Sun, Y. N. Zeng, D. Wang, W. J. Zhang, Y. Li, *Organometallics* **2010,** *29*, 2459–2464.

16 R. K. J. Bott, D. L. Hughes, M. Schormann, M. Bochmann, S. J. Lancaster, *J. Organomet. Chem.* **2003,** *665*, 135–149.

17 (a) S. R. Liu, B. X. Li, J. Y. Liu, Y. S. Li, *Polymer* **2010,** *51*, 1921–1925; (b) J. Y. Liu, S. R. Liu, B. X. Li, Y. G. Li, Y. S. Li, *Organometallics* **2011,** *30*, 4052–4059.

18 C. H. Qi, S. B. Zhang, J. H. Sun, *J. Organomet. Chem.* **2005,** *690*, 2941–2946.

19 C. A. Willoughby, R. R. Duff Jr., W. M. Davis, S. L. Buchwald, *Organometallics* **1996,** *15*, 472–475.

20 (a) J. Zhang, Y. J. Lin, G. X. Jin, *Organometallics* **2007,** *26*, 4042–4047; (b) P. Hu, Y. J. Lin, G. X. Jin, *Organometallics* **2011,** *30*, 1008–1012.

21 (a) R. J. Long, V. C. Gibson, A. J. P. White, D. J. Williams, *Inorg. Chem.* **2006,** *45*, 511–513; (b) R. J. Long, V. C. Gibson, A. J. P. White, *Organometallics* **2008,** *27*, 235–245.

22 L. P. He, J. Y. Liu, Y. G. Li, S. R. Liu, Y. S. Li, *Macromolecules* **2009,** *42*, 8566–8570.

23 (a) E. J. Baerends, D. E. Ellis, P. Ros, *Chem. Phys.* **1973,** *2*, 41–51; (b) E. J. Baerends, P. Ros, *Chem. Phys.* **1973,** *2*, 52–59.

24 A. D. Becke, *Phys. Rev. A* **1988,** *38*, 3098–3100.

25 J. P. Perdew, *Phys. Rev. B* **1986,** *33*, 8822–8824.

26 (a) P. Gomez-Sal, A. Martin, M. Mena, P. Royo, R. Serrano, *J. Organomet. Chem.* **1991,** *419*, 77–84; (b) M. G. Thorn, J. S. Vilardo, J. Lee, B. P. Hanna, E. Fanwick, I. P. Rothwell, *Organometallics* **2000,** *19*, 5636–5642.

27 E. Y. X. Chen, T. J. Marks, *Chem. Rev.* **2000,** *100*, 1391–1434.

28 S. Matsui, M. Mitani, J. Saito, Y. Tohi, H. Makio, N. Matsukawa, Y. Takagi, K. Tsuru, M. Nitabaru, T. Nakano, H. Tanaka, N. Kashiwa, T. Fujita, *J. Am. Chem. Soc.* **2001,** *123*, 6847–6856.

29 (a) A. L. McKnight, R. M. Waymouth, *Macromolecules* **1999,** *32*, 2816–2825; (b) T. Hasan, T. Ikeda, T. Shiono, *Macromolecules* **2004,** *37*, 8503–8509.

30 (a) P. Altamura, A. Grassi, *Macromolecules* **2001,** *34*, 9197–9200; (b) Y. Yoshida, J. Saito, M. Mitani, Y. Takagi, S. Matsui, S. Ishii, T. Nakano, N. Kashiwa, T. Fujita, *Chem. Commun.* **2002**, 1298–1299; (c) Y. Yoshida, J. Mohri, S. Ishii, M. Mitani, J. Saito, S. Matsui, H. Makio, T. Nakano, H. Tanaka, M. Onda, Y. Yamamoto, A. Mizuno, T. Fujita, *J. Am. Chem. Soc.* **2004,** *126*, 12023–12032; (d) X. F. Li, K. Dai, W. P. Ye, L. Pan, Y. S. Li, *Organometallics* **2004,** *23*, 1223–1230.

31 (a) D. Ruchatz, G. Fink, *Macromolecules* **1998,** *31*, 4669–4673; (b) D. Ruchatz, G. Fink, *Macromolecules* **1998,** *31*, 4674–4680; (c) D. Ruchatz, G. Fink, *Macromolecules* **1998,** *31*, 4681–4683; (d) D. Ruchatz, G. Fink, *Macromolecules* **1998,** *31*, 4684–4686.

32 (a) A. Provasoli, D. R. Ferro, I. Tritto, L. Boggioni, *Macromolecules* **1999,** *32*, 6697–6706; (b) I. Tritto, C. Marestin, L. Boggioni, L. Zetta, A. Provasoli, D. R. Ferro, *Macromolecules* **2000,** *33*, 8931–8944; (c) I. Tritto, C. Marestin, L. Boggioni, M. C. Sacchi, H. H. Brintzinger, D. R. Ferro, *Macromolecules* **2001,** *34*,

5770–5777; (d) I. Tritto, L. Boggioni, J. C. Jansen, K. Thorshaug, M. C. Sacchi, D. R. Ferro, *Macromolecules* **2002,** *35*, 616–623; (e) K. Thorshaug, R. Mendichi, L. Boggioni, I. Tritto, S. Trinkle, C. Friedrich, R. Mülhaupt, *Macromolecules* **2002,** *35*, 2903–2911; (f) I. Tritto, L. Boggioni, D. R. Ferro, *Macromolecules* **2004,** *37*, 9681–9693.

33 (a) P. Cossee, *J. Catal.* **1964,** *3*, 80–88; (b) M. Brookhart, M. L. H. Green, *J. Organomet. Chem.* **1983,** *250*, 395–408.

34 A. Laine, M. Linnolahti, T. A. Pakkanen, J. R. Severn, E. Kokko, A. Pakkanen, *Organometallics* **2010,** *29*, 1541–1550.

35 E. G. Kim, M. L. Klein, *Organometallics* **2004,** *23*, 3319–3326.

36 G. Lanza, I. L. Fragalá, T. J. Marks, *Organometallics* **2002,** *21*, 5594–5612.

37 M. Dahlmann, G. Erker, K. Bergander, *J. Am. Chem. Soc.* **2000,** *122*, 7986–7998.